Dilepton distributions at backward rapidities

M. A. Betemps,[1,2,*] M. B. Gay Ducati,[1,†] and E. G. de Oliveira[1,‡]

[1]*High Energy Physics Phenomenology Group (GFPAE), Instituto de Física, Universidade Federal do Rio Grande do Sul, Caixa Postal 15051, CEP 91501-970, Porto Alegre, RS, Brazil*

[2]*Conjunto Agrotécnico Visconde da Graça, CAVG, Universidade Federal de Pelotas, Caixa Postal 460, CEP 96060-290, Pelotas, RS, Brazil*

(Received 31 July 2006; published 10 November 2006)

The dilepton production at backward rapidities in pAu and pp collisions at RHIC and LHC energies is investigated in the dipole approach. The results are shown through the nuclear modification ratio R_{pA} considering transverse momentum and rapidity spectra. The dilepton modification ratio presents interesting behavior at the backward rapidities when compared with the already known forward ones, since it is related with the large x kinematical region that is being probed. The rapidity dependence of the nuclear modification ratio in the dilepton production is strongly dependent on the Bjorken x behavior of the nuclear structure function ratio $R_{F_2} = F_2^A/F_2^p$. The R_{pA} transverse momentum dependence at backward rapidities is modified due to the large x nuclear effects: at RHIC energies, for instance, the ratio R_{pA} is reduced as p_T increases, presenting an opposite behavior when compared with the forward one. It implies that the dilepton production at backward rapidities should carry information of the nuclear effects at large Bjorken x, as well as that it is useful to investigate the p_T dependence of the observables in this kinematical regime.

DOI: 10.1103/PhysRevD.74.094010 PACS numbers: 12.38.−t, 13.85.Qk

I. INTRODUCTION

The hadron transverse momentum spectrum measured by the RHIC experiments [1] is one of the most accessible distributions carrying information about the high density nuclear environment. At forward rapidities, the transverse momentum distribution for hadrons presents results compatible with the Color Glass Condensate (CGC) description of the saturated regime at high energies [2]. These results are investigated through a nuclear modification ratio, which relates dAu and pp collisions. It is well known that the transverse momentum dependence of this ratio shows a pronounced Cronin peak at central rapidity, which is suppressed at forward ones. For central rapidities the Cronin peak is due to the multiple scatterings of the projectile constituents with the dense target. At large rapidities the Cronin peak suppression is understood as a signal of the saturation phenomena intrinsic of the Color Glass Condensate (CGC). However, at backward rapidities, the recently measured hadron nuclear modification ratio shows a pronounced peak [3], which should be due to final states interactions.

In this work the dilepton production at high energies in the backward rapidity region is investigated in the proton-nucleus and proton-proton collisions. The analysis at forward rapidities was already done [4] and the results show that the dilepton is also a suitable observable to investigate the Color Glass Condensate. Here, the interest to explore the backward region in the dilepton sector relies on the study of the nuclear effects at large and small x and on the comparison with the Cronin effect in this region. In this kinematical region, the nucleus interacts by means of large Bjorken x partons, and no saturation effects are expected consequently. In this regime, the proton interacts through the small x partons.

It has been shown [4] that the dilepton production at forward rapidities, analyzed in the context of the Color Glass Condensate in pAu collisions, presents the same features of the Cronin effect at forward rapidities, implying that this should be considered as an initial state effect. However, at backward rapidities, the Cronin peak present in the hadrons RHIC data [3] is still not understood, and could be related to final state effects. The dileptons analyzed in this kinematical region, since they do not interact strongly with the final environment, may not present the same behavior of the hadron spectra. Although it could imply the dilepton production to be symmetric when forward-backward regions are compared, in contrast to the different behavior of the hadron spectra in both regions, we verify that the dilepton production at backward rapidities is strongly modified due to large x nuclear effects.

This work is organized as follows. In the next section the dipole approach is presented for the dilepton production at backward rapidities. In the Sec. III the nuclear partonic parametrizations employed in this work as well as a comparison between then are presented. In the Sec. IV4 the results are discussed. Our conclusions are left to the last section of this work.

II. DILEPTON PRODUCTION AT BACKWARD RAPIDITIES

To evaluate the dilepton production at backward rapidities, an adequate treatment of the approach employed for

*Electronic address: marcos.betemps@ufrgs.br
†Electronic address: beatriz.gay@ufrgs.br
‡Electronic address: emmanuel.deoliveira@ufrgs.br

the forward ones needs to be considered. The investigation at forward rapidities in pA collisions requires to describe the nucleus as a high density saturated system (CGC), and the dileptons are produced by the decay of a virtual photon emitted by the quark from the proton, which interacts with the nuclear dense medium (basically a dipole approach in the momentum space with a specific configuration of the nucleus). In this case the dilepton cross section can be factorized considering the wave function of the fluctuation $q\gamma^*$ and the interaction cross section of a quark with the nucleus, which takes into account the high density effects. However, at backward rapidities the nucleus interacts by means of large Bjorken x partons, being no more described by a high density QCD system. The proton interacts through very small x partons implying that the dipole picture could be applied in this kinematical regime.

In the dipole approach at backward rapidities, the quark of the incident hadron (nucleus) fluctuates into a state containing a quark and a massive photon. The interaction with the target (proton) provides that the virtual photon is freed, decaying into a lepton pair [5] (one of the diagrams is shown in the Fig. 1).

We are interested in the study of the dilepton production in a region where the interaction time of the projectile quark with the proton target is much shorter than the $q\gamma^*$ fluctuation time, meaning large coherence length. In order to apply the dipole picture at backward rapidities, we need to exchange the nucleus with the proton when comparing with the dipole picture at forward rapidities. In doing such procedure, the $q\gamma^*$ fluctuation time will be larger than the interaction time, since the coherence length l_c has the dependence $l_c \propto 1/x_1$ in the case studied here. Indeed, the coherence length is important in the study of nuclear targets, where it is a fundamental quantity controlling nuclear effects [6]. For the nuclear targets large coherence length needs to be reached if shadowing effect are under investigation, which implies that the approach should be applied only to smaller Bjorken x [7]. Another interesting point that arises here is that the p_T broadening due to the nuclear multiple scattering verified at forward rapidities [6] should not be present at backward rapidities, since the nuclear projectile will interact with a proton target and will not probe a large and very dense system.

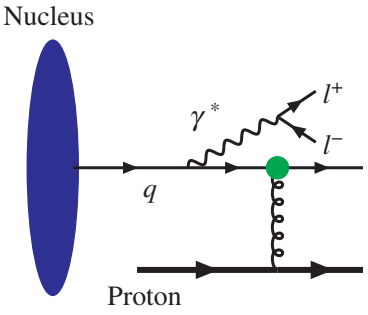

FIG. 1 (color online). In the dipole approach, dilepton production looks like a bremsstrahlung. A quark or an antiquark from the projectile hadron (nucleus) scatters off the target color field and radiates a photon (γ^*) with mass M (before or after the quark scatters), which subsequently decays into the lepton pair.

The advantage of this formalism is that the dilepton cross section can be written in terms of the same color dipole cross section as small-x Deep Inelastic Scattering (DIS). Although diagrammatically no dipole is present in bremsstrahlung, the dipole cross section arises from the interference of the two bremsstrahlung diagrams, as shown in Ref. [8] in a detailed derivation.

The cross section for the radiation of a virtual photon from a quark (with momentum fraction x_2) of the nucleus scattering off a proton at high density at backward region can be written in a factorized form as [9,10],

$$\frac{d\sigma^{DY_{\text{back}}}}{dM^2 dy d^2p_T} = \frac{\alpha_{em}^2}{6\pi^3 M^2}\int_0^\infty d\rho W(x_2, \rho, p_T)\sigma_{\text{dip}}(x_1, \rho), \tag{1}$$

where p_T is the dilepton transverse momentum, M is the dilepton mass, y the rapidity, ρ is the dipole transverse separation. The variables x_1 and x_2 are defined in the usual way

$$x\begin{pmatrix}1\\2\end{pmatrix} = \sqrt{\frac{M^2 + p_T^2}{s}}e^{\pm y},$$

with s being the squared center of mass energy. As can be seen from the definition of x_1 and x_2, backward rapidities will provide large x_2 and small x_1. We are investigating dilepton production in pp and pA collisions. In a symmetric collision, the lab frame is equivalent to the center of mass frame considering colliders. In the case of asymmetric collisions, e.g. pA, the center of mass moves longitudinally in the lab frame. It provides that a largest interval in Bjorken x could be explored in the asymmetric collisions [11] if the lab frame is under consideration. In this work the ratio between pA and pp collisions will be investigated considering the rapidity in the lab frame.

Based on the dipole approach, the function $W(x_2, \rho, p_T)$ is given by [9],

$$\begin{aligned} W(x_2, \rho, p_T) = \int_{x_2}^1 \frac{d\alpha}{\alpha^2} F_2^A\left(\frac{x_2}{\alpha}, M^2\right)\Big\{[m_q^2\alpha^2 + 2M^2(1-\alpha)^2] \\ \times\left[\frac{1}{p_T^2 + \eta^2}T_1(\rho) - \frac{1}{4\eta}T_2(\rho)\right] \\ + [1 + (1-\alpha)^2]\left[\frac{\eta p_T}{p_T^2 + \eta^2}T_3(\rho) - \frac{1}{2}T_1(\rho) \right. \\ \left. + \frac{\eta}{4}T_2(\rho)\right]\Big\}. \end{aligned} \tag{2}$$

In the above equation α is the momentum fraction of the quark carried by the virtual photon, $\eta^2 = (1-\alpha)M^2 + \alpha^2 m_q^2$, m_q is the quark mass ($m_q = 0.2$ GeV) and the

functions T_i are given by,

$$T_1(\rho) = \frac{\rho}{\alpha} J_0\left(\frac{p_T\rho}{\alpha}\right) K_0\left(\frac{\eta\rho}{\alpha}\right)$$

$$T_2(\rho) = \frac{\rho^2}{\alpha^2} J_0\left(\frac{p_T\rho}{\alpha}\right) K_1\left(\frac{\eta\rho}{\alpha}\right)$$

$$T_3(\rho) = \frac{\rho}{\alpha} J_1\left(\frac{p_T\rho}{\alpha}\right) K_1\left(\frac{\eta\rho}{\alpha}\right).$$

Here, a nuclear structure function $F_2^A(\frac{x_2}{\alpha}, M^2)$ with a x_2 dependence is considered in order to take into account the nuclear interaction. For pp collisions the nuclear structure function $F_2^A(\frac{x_2}{\alpha}, M^2)$ needs to be replaced by the proton structure function $F_2^p(\frac{x_2}{\alpha}, M^2)$. The dipole cross section is evaluated with the argument x_1 and the same dipole cross section extracted from the deep inelastic scattering HERA data should be applied.

The dipole cross section in the phenomenological model proposed by Golec-Biernat and Wüsthoff [12] (GBW), which has produced a good description of HERA data in both inclusive and diffractive processes, was employed here. It is constructed interpolating the color transparency behavior $\sigma_{\rm dip} \sim \rho^2$ for small dipole sizes and a flat (saturated) behavior for large dipole sizes $\sigma_{\rm dip} \sim \sigma_0$ (confinement). The expression has the eikonal-like form,

$$\sigma_{\rm dip}(x_1, \rho) = \sigma_0\left[1 - \exp\left(-\frac{\rho^2 Q_0^2}{4(x_1/x_0)^\lambda}\right)\right], \qquad (3)$$

where $Q_0^2 = 1$ GeV^2 and the three fitted parameters are $\sigma_0 = 23.03$ mb, $x_0 = 3.04 \times 10^{-4}$ and $\lambda = 0.288$.

The pp and pAu transverse momentum distributions at RHIC energies for backward rapidities can now be evaluated, considering a specific parametrization to the nuclear structure function $F_2^A(x, M^2)$ in the pA case. Two distinct parametrizations for the nuclear structure function will be used, which will be properly discussed in the next section. In this section EKS nuclear parametrization [13] was employed together with the GRV98 parton distribution function [14] in order to obtain the p_T distribution for the pA collision and the $F_2^p(x, M^2)$ is obtained from the GRV98 parametrization for the pp collision. In the Fig. 2 the pp and pA transverse momentum distributions for RHIC energies are shown and significative visible differences between both distributions are not found. For this reason, the ratio between pA and pp cross section should be useful to investigate modifications in the nuclear cross section in comparison with the pp distribution. The ratio is defined in the following way

$$R_{pA} = \frac{d\sigma(pA)}{dp_T^2 dy dM} \Big/ A\frac{d\sigma(pp)}{dp_T^2 dy dM}. \qquad (4)$$

The ratio R_{pA} is normalized by $1/A$, since the nuclear parton distributions are normalized by this factor. The difference between pA and pp calculations are due to the nuclear structure function F_2^A, then any effect in the p_T or rapidity spectra should be related to the nuclear effects contained in this function.

The next-to-leading-order calculation (NLO) in the collinear factorization could be evaluated and compared with the results in the dipole approach. However, the evaluation of the transverse momentum distribution in the collinear factorization is not a straightforward calculation and does not describe the normalization of the p_T Drell-Yan dileptons [15,16]. A resummation of large logarithms in p_T/M [15,16] or the introduction of an intrinsic transverse momentum [17] should be necessary to avoid the divergence of the differential cross section at $p_T \ll M$. New approaches have been suggested in order to describe the p_T spectra of the dilepton (for a good discussion see Ref. [18]), however, there is a strong dependence on phenomenological parameters. Considering, for instance, the intrinsic transverse momentum, the p_T distribution is dependent on a phenomenological parameter (see Ref. [8] for a comparison between the NLO calculations and the dipole approach, and Ref. [18] for a new approach). Of course, the ratio R_{pA} should be finite since the p_T divergence will be canceled, however, a more reliable result needs to consider finite spectra. This indicates that the dipole approach should be more adequated to investigate the low p_T dilep-

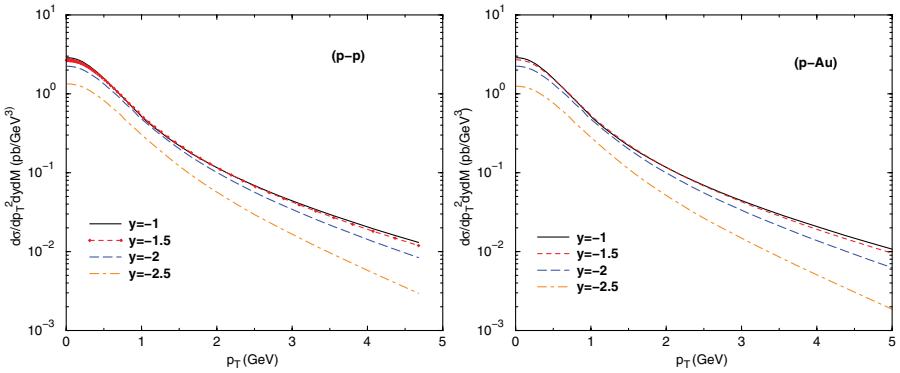

FIG. 2 (color online). Dilepton transverse momentum distribution for pp and pA (Au—considering EKS parametrization) collision at RHIC energies for dilepton mass $M = 6$ GeV.

tons at high energies, since there are no free parameters and the cross section is finite at low p_T.

For sake of completeness, it should be stressed that some limitations of the dipole approach at backward rapidities are in order. Here, the nucleus is considered by means of an integrated gluon distribution, however, at LHC energies and more central rapidities, the Bjorken x_2 (nucleus) reaches values around 0.002, where the consideration of an integrated parton distribution could be questionable. At this high energy limit, the effects of finite transverse momentum of the incoming partons become important. A more robust treatment would need to include the transverse momentum of the partons from the nucleus in the initial state of the interaction. This should be done considering the k_T factorization approach [19], where the off-shell partonic cross sections are convoluted with k_T unintegrated parton densities $f_a(x, k_T^2, \mu^2)$. Considering dilepton production, the k_T factorization is investigated in the Ref. [20] and compared with a phenomenological intrinsic k_T approach (k_T factorization with on-shell partons), in order to describe the transverse momentum distribution of the Drell-Yan dilepton production. In spite of a reasonable data description, the k_T factorization overestimates the data and the intrinsic k_T approach depends on phenomenological parameters (two parameters).

For the reasons presented above, we have focused our analysis at backward rapidities, and not at more central ones. The use of the dipole approach together with the collinear factorization is justified as the goal of this work is to investigate the nuclear effects in the nuclear modification ratio R_{pA} for dileptons, using nuclear parametrizations to describe the F_2^A. In the next section the parametrizations for the nuclear structure function will be discussed and compared.

III. NUCLEAR PARTON DISTRIBUTION FUNCTION

In this work the parametrizations for the nuclear parton distribution function (nPDF) proposed by Eskola, Kolhinen and Salgado (EKS parametrization) [13] and by D. de Florian and R. Sassot (nDS parametrization) [21] are considered in order to describe the nuclear effects in the F_2^A. In this section the main features of each parametrization will be discussed.

Both nuclear parton distribution functions provide a global fitting to fixed target experimental results, and consider the DGLAP equations for the Q^2 evolution. The initial conditions are adjusted to describe the DIS in lepton-nucleus collisions and the dilepton production in proton-nucleus collisions. Both nPDFs are used to obtain an appropriated parametrization for the ratio $R_{F_2}^A(x, Q_0^2) = F_2^A/AF_2^p$, with

$$F_2^{A,p} = \sum_q e_q^2 [x f_q^{A,p}(x, Q_0^2) + x f_{\bar{q}}^{A,p}(x, Q_0^2)], \qquad (5)$$

in which $f_q^p(x, Q_0^2)$ are the free proton parton distributions and $f_q^A(x, Q_0^2)$ are the nuclear distributions of parton flavor q. The parametrization for the parton distributions are constrained by charge, baryon number, and momentum conservation.

However, the method used by EKS and nDS differs with respect to their approaches to parametrize the nPDFs. In the EKS approach, the nuclear parton distributions are the free proton ones times a correction factor: $f_q^A(x, Q_0^2) = R_q^A(x, Q_0^2) f_q^p(x, Q_0^2)$, and all nuclear effects are enclosed in $R_q^A(x, Q_0^2)$. One consequence of this definition is that the nPDFs are null for $x > 1$, although they should be nonzero for $x < A$. On the other hand, nDS uses a convolution to relate nPDFs to the free proton PDFs:

$$f_q^A(x, Q_0^2) = \int_x^A \frac{dy}{y} W_q(y, A) f_q^p\left(\frac{x}{y}, Q_0^2\right), \qquad (6)$$

in which $W_i(y, A)$ contains the information about the nuclear effects. For instance, if nuclear effects are disconsidered, $W_q(y, A) = A\delta(1 - y)$.

The nuclear effects are verified by comparison of the nuclear structure function with the proton (or deuterium) structure function. In the Fig. 3 the prediction for the ratio F_2^A/AF_2^p is presented for both parametrizations. The figure can be divided in four regions of Bjorken-x [22]. In the Fermi motion region $x \gtrsim 0.8$, $R_{F_2}^A$ is greater than 1 and increases with x. The EMC region $0.3 \lesssim x \lesssim 0.8$ is characterized by $R_{F_2}^A < 1$. The antishadowing region $0.1 \lesssim x \lesssim 0.3$, and the shadowing region $x \lesssim 0.1$ are defined by $R_{F_2}^A > 1$, and $R_{F_2}^A < 1$, respectively. The Fig. 3 shows that the parametrizations differ most in both ECM and shadowing regions, with EKS parametrization getting a

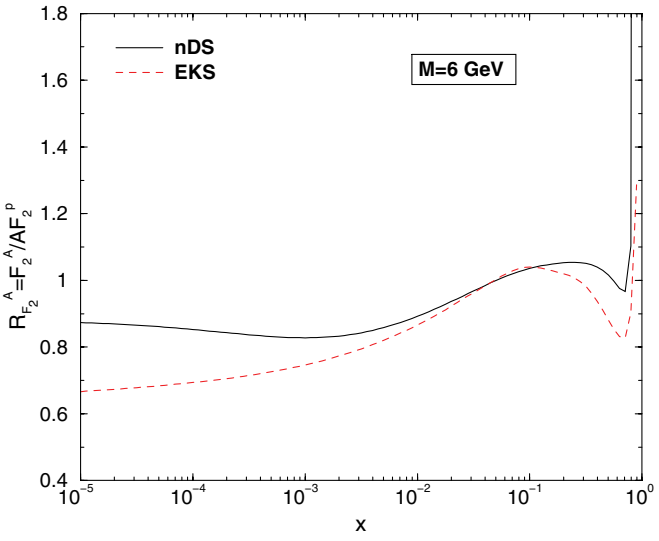

FIG. 3 (color online). Comparison between EKS and nDS parametrizations for the ratio F_2^A/F_2^p (A = Au) for a dilepton mass (scale) $M = 6$ GeV as a function of the Bjorken x of the nucleus.

lower ratio than nDS. The parametrizations are considered at the leading-order, since the approach employed here considers LO diagrams, without higher orders calculations. Indeed, the dipole cross section should carry some information about higher orders, but these properties are included in the phenomenological parametrization of the dipole cross section, in our case, the GBW parametrization [12].

In the next section, the results for dilepton production will be explored, considering both parametrizations for the nuclear parton distribution presented in this section.

IV. RESULTS AND DISCUSSIONS

The results for transverse momentum and rapidity distributions for the dilepton production (with mass $M = 6$ GeV) at RHIC ($\sqrt{s} = 200$ GeV) and LHC ($\sqrt{s} = 8.8$ TeV) energies at backward rapidities will be discussed.

The ratio R_{pA} was evaluated at RHIC and LHC energies, and in the Figs. 4 and 5 the results are shown in 3D plots for rapidity and p_T spectra, considering the EKS and nDS parametrizations. The behavior of the ratio R_{pA} reflects the x_2 dependence of the ratio F_2^A/F_2^p, presented in the Fig. 3.

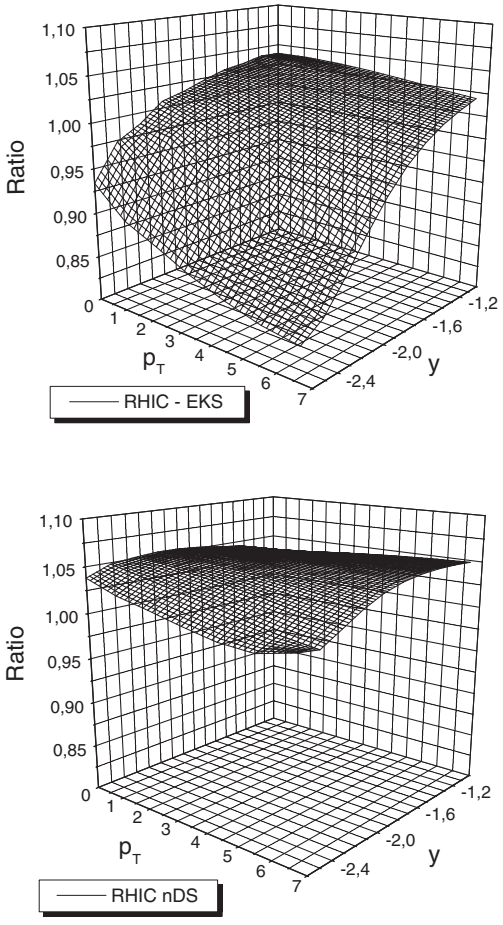

FIG. 4. Ratio R_{pA} for RHIC energies considering the EKS and nDS parametrizations.

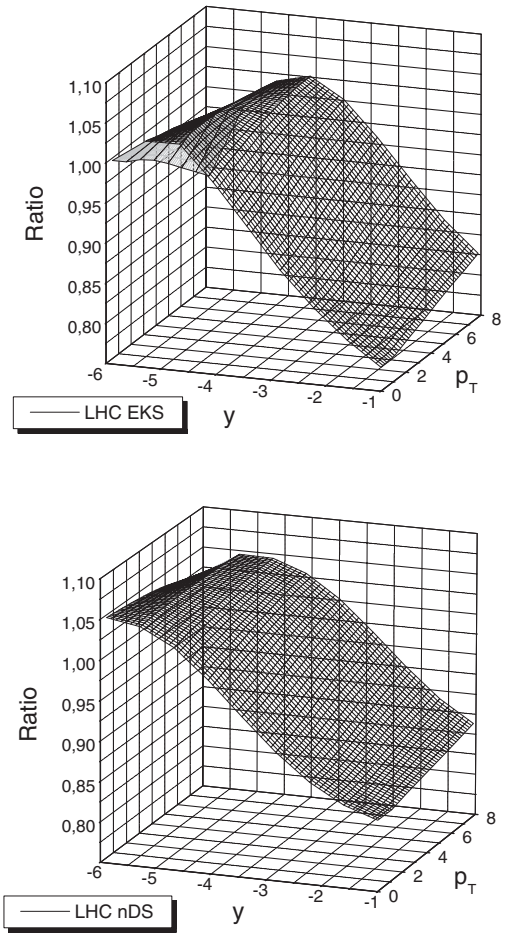

FIG. 5. Ratio R_{pA} for LHC energies considering the EKS and nDS parametrizations.

At RHIC energies a weak dependence of the ratio on the transverse momentum is verified, and in general the ratio reaches smaller values at large p_T, being this more evident with the EKS parametrization. Concerning the rapidity spectra, the EKS parametrization predicts a strong suppression of the ratio at very backward rapidities and large p_T, in comparison with the nDS parametrization, which predicts an almost flat behavior.

To explain such results it is necessary to know the range of x_2 values in the rapidity and p_T spectra at RHIC. For RHIC energies considering rapidities from -1 to -2.6, and p_T from 1 to 7, the x_2 range is between 0.08 and 0.5, respectively, meaning that for more backward rapidities, partons with larger x_2 are being probed. The nuclear effects that appear in the F_2^A at this x_2 range are mainly due to EMC effect (reduction of the ratio $R_{F_2}^A$ as x_2 increases, see Fig. 3), which provides the reduction of the ratio R_{pA} at lower rapidities in the Fig. 4. Concerning the p_T spectra, x_2 increases with p_T, and as the region probed here is related to the EMC effect, the result is a reduction of the ratio R_{pA}

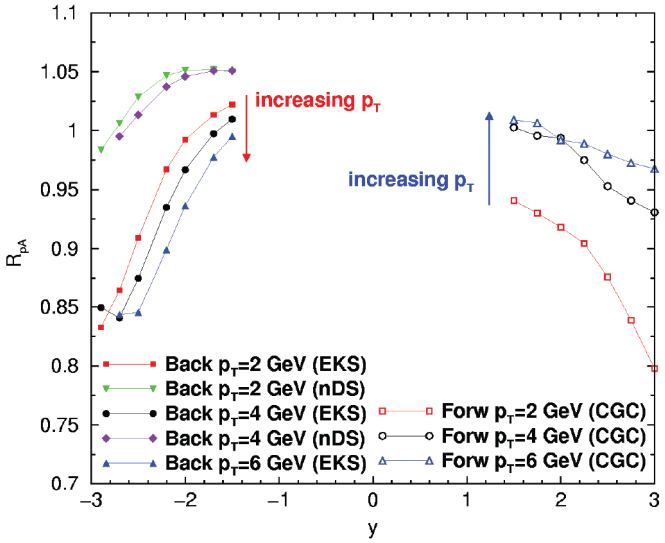

FIG. 6 (color online). Comparing the ratio R_{pA} for dileptons at backward and forward rapidities for RHIC energies, considering the EKS and nDS nuclear parametrizations at backward, and the CGC predictions at forward [4].

as p_T increases. The large suppression of the ratio R_{pA} of the EKS prediction in comparison with the nDS in the Fig. 4 is a consequence of the large difference in the $R^A_{F_2}$ predictions of the parametrizations in the EMC effect region.

At LHC energies (Fig. 5) the rapidity spectra present a peak at intermediated rapidities, which is more pronounced in the EKS parametrization in comparison with the nDS parametrization. The R_{pA} transverse momentum dependence presents two distinct behaviors: for very backward rapidities the ratio decreases as p_T increases and for more central rapidities the ratio R_{pA} increases with p_T.

For LHC energies, rapidities from -1 to -6, and p_T from 1 to 7, the x_2 range is between 0.002 and 0.3, respectively. Here we verify that not only large x of the nucleus is been probed, but small x too. The x_2 range probed at LHC provides that shadowing and antishadowing effects are present. The peak at intermediate rapidities is related to the antishadowing effect and the suppression at more central rapidities is related to the shadowing effect. The p_T spectra is more involved since the ratio R_{pA} presents different behaviors. For more backward rapidities the ratio is reduced for large p_T (x_2 in the antishadowing region, near to EMC region). For more central rapidities, the ratio increases for large p_T, since the x_2 is in the shadowing region.

Comparing the predictions from the EKS and nDS parametrizations, in the Fig. 3 the EKS parametrization predicts more pronounced antishadowing, which explains the results found here for the ratio R_{pA} at LHC energies (Fig. 5). Our results presented for LHC energies show that dilepton carries information about the large and small x regime of the nuclear environment. The distinct nuclear effects are verified in rapidity and p_T spectra for the dilepton production at backward rapidities, for RHIC and LHC energies, following the x region involved.

In order to compare the results presented in this work, with the previous results from the forward region [4], in the Fig. 6 the ratio R_{pA} for RHIC energies is shown for positive and negative rapidities. The ratio presents different behaviors concerning the transverse momentum dependence. While at forward rapidities the saturation phenomena implies that the ratio R_{pA} increases at large p_T, at backward rapidities the ratio R_{pA} decreases as large p_T is reached. This distinct behavior is associated with the large x nuclear effects present at backward rapidities.

V. CONCLUSIONS

The nuclear modification ratio R_{pA} for the dilepton production was investigated for p_T and backward rapidity spectra in the dipole picture for RHIC and LHC energies. We have verified a strong dependence of the nuclear modification ratio with the nuclear effects. The results presented in this work are explained by the dependence of the nuclear structure function ratio $R^A_{F_2}$ on the Bjorken x. The hadron production was investigated at backward rapidities by PHENIX collaboration at RHIC [3] presenting the data on the nuclear modification ratio. The results present an enhancement in the nuclear modification ratio for $1.5 < p_T < 4.0$, which still demands some caution, once there are some data uncertainties and a discrepancy between analysis methods of the data. The results presented in this work for dileptons indicate that the enhancement in the hadron spectra at backward rapidities could be mainly due to final states, since, the initial state effects investigated here do not provide such behavior. Moreover, the dilepton at backward rapidities is a suitable observable to understand and quantify the nuclear effects at large and small Bjorken x. Additionally, the transverse momentum dependence of the ratio R_{pA} is strongly modified at RHIC energies, if forward and backward rapidities are compared, due to distinct x regions being probed.

ACKNOWLEDGMENTS

We thank Boris Kopeliovich for fruitful discussions during his visit to GFPAE at the occasion of the I LAWHEP and for a careful reading of this manuscript. This work was partially supported by CNPq, Brazil.

[1] R. Debbe (BRAHMS collaboration), J. Phys. G **30**, S759 (2004); I. Arsene *et al.* (BRAHMS Collaboration), Phys. Rev. Lett. **93**, 242303 (2004).
[2] J. Jamal-Jalilian and Y. Kovchegov, Prog. Part. Nucl. Phys. **56**, 104 (2006).
[3] S. S. Adler *et al.* (PHENIX Collaboration), Phys. Rev. Lett. **94**, 082302 (2005).
[4] M. A. Betemps and M. B. Gay Ducati, Phys. Rev. D **70**, 116005 (2004); Eur. Phys. J. C **43**, 365 (2005); Phys. Lett. B **636**, 46 (2006).F. Gelis and J. Jalilian-Marian, Phys. Rev. D **66**, 094014 (2002).R. Baier, A. H. Mueller, and D. Schiff, Nucl. Phys. A **741**, 358 (2004).
[5] B. Z. Kopeliovich, J. Raufeisen, A. V. Tarasov, and M. B. Johnson, Phys. Rev. C **67**, 014903 (2003).
[6] M. B. Johnson *et al.*, hep-ph/0606126.
[7] N. Armesto, Eur. Phys. J. C **26**, 35 (2002).
[8] J. Raufeisen, J. C. Peng, and G. C. Nayak, Phys. Rev. D **66**, 034024 (2002).
[9] M. A. Betemps, M. B. Gay Ducati, M. V. T. Machado, and J. Raufeisen, Phys. Rev. D **67**, 114008 (2003).
[10] B. Z. Kopeliovich, in *Proceedings of Workshop Hirschegg'95: Dynamical Properties of Hadrons in Nuclear Matter*, Edited by H. Feldmeier and W. Nörenberg (GSI, Darmstadt, 1995), p. 102; S. J. Brodsky, A. Hebecker, and E. Quack, Phys. Rev. D **55**, 2584 (1997).
[11] N. Carrer and A. Daianese, Report No. ALICE-INT-2003-019.
[12] K. Golec-Biernat and M. Wüsthoff, Phys. Rev. D **59**, 014017 (1998); **60**, 114023 (1999).
[13] K. J. Eskola, V. J. Kolhinen, and C. A. Salgado, Eur. Phys. J. C **9**, 61 (1999); K. J. Eskola, V. J. Kolhinen, and P. V. Ruuskanen, Nucl. Phys. **B535**, 351 (1998).
[14] M. Glück, E. Reya, and A. Vogt, Eur. Phys. J. C **5**, 461 (1998).
[15] J. C. Collins, D. E. Soper, and G. Sterman, Nucl. Phys. **B250**, 199 (1985).J. W. Qiu and X. F. Zhang, Phys. Rev. Lett. **86**, 2724 (2001).
[16] G. I. Fai, J. W. Qiu, and X. F. Zhang, Phys. Lett. B **567**, 243 (2003).
[17] G. Altarelli, G. Parisi, and R. Petronzio, Phys. Lett. B **76**, 351 (1978).
[18] O. Linnyk, S. Leupold, and U. Mosel, hep-ph/0607305.
[19] S. Catani, M. Ciafaloni, and F. Hautmann, Phys. Lett. B **242**, 97 (1990); Nucl. Phys. **B366**, 135 (1991).J. Collins and R. Ellis, Nucl. Phys. **B360**, 3 (1991).
[20] O. Linnyk, S. Leupold, and U. Mosel, Phys. Rev. D **71**, 034009 (2005).
[21] D. de Florian and R. Sassot, Phys. Rev. D **69**, 074028 (2004).
[22] N. Armesto, hep-ph/0604108.